

# Fundamental Limits of Large Momentum Transfer in Optical Lattices

Ashkan Alibabaei,<sup>1,\*</sup> Patrik Mönkeberg,<sup>2,\*</sup> Florian Fitzek,<sup>1,2,†</sup> Alexandre Gauguet,<sup>3</sup> Baptiste Allard,<sup>3</sup> Klemens Hammerer,<sup>2,4,5,‡</sup> and Naceur Gaaloul<sup>1,§</sup>

<sup>1</sup>*Institute of Quantum Optics, Leibniz University of Hannover, Welfengarten 1 30167 Hannover, Germany*

<sup>2</sup>*Institute of Theoretical Physics, Leibniz University of Hannover, Appelstrasse 2 30167 Hannover, Germany*

<sup>3</sup>*Laboratoire Collisions Agrégats Réactivité, FERMI,*

*Université de Toulouse and CNRS UMR5589, 118 Route de Narbonne, F-31062 Toulouse, France*

<sup>4</sup>*Institute for Theoretical Physics, University of Innsbruck, 6020 Innsbruck, Austria*

<sup>5</sup>*Institute for Quantum Optics and Quantum Information of the Austrian Academy of Sciences, 6020 Innsbruck, Austria*

(Dated: February 3, 2026)

Large-momentum-transfer techniques are instrumental for the next generation of atom interferometers as they significantly improve their sensitivity. State-of-the-art implementations rely on elastic scattering processes from optical lattices such as Bloch oscillations or sequential Bragg diffraction, but their performance is constrained by imperfect pulse efficiencies. Here we develop a Floquet-based theoretical framework that provides a unified description of elastic light-atom scattering across all relevant regimes. Within this formalism, we identify practical regimes that exhibit orders of magnitude reduced losses and improved phase accuracy compared to previous implementations. The model's validity is established through direct comparison with exact numerical solutions of the Schrödinger equation and through quantitative agreement with recent experimental benchmark results. These findings delineate previously unexplored operating regimes for large-momentum-transfer beam splitters and open new perspectives for precision atom-interferometric measurements in fundamental physics, gravity gradiometry or gravitational wave detection.

**Introduction**— Atom Interferometry (AI) has proven to be a highly sensitive and accurate tool for quantum sensing [1] advancing inertial navigation [2, 3], precision measurements [4–7], fundamental constants determination [8–10] and tests of general relativity [11, 12].

One way to enhance the sensitivity of an atom interferometer is to increase the spatial separation between the arms with sizable photon exchange, a technique known as Large Momentum Transfer (LMT)[13–16]. Methods to realize LMT include single photon transitions [17], Raman diffraction [18, 19], as well as elastic-scattering in optical lattices such as Bloch oscillation (BO) [20–23] and Sequential Bragg Diffraction (SBD) [24, 25] as illustrated in Fig. 1.

Recently, momentum separations of up to 600 photon recoils have been achieved using SBD [25], exceeding earlier 400 photon recoils in BO-based implementations [23]. These results naturally raise the questions of whether BO and SBD represent fundamentally distinct elastic scattering mechanisms, and how their respective efficiency and accuracy compare under given experimental constraints and whether either approach can be extended to reach momentum separations on the order of several thousand photon recoils as required for next-generation atom-interferometric sensors detecting gravitational waves or investigating the nature of dark energy

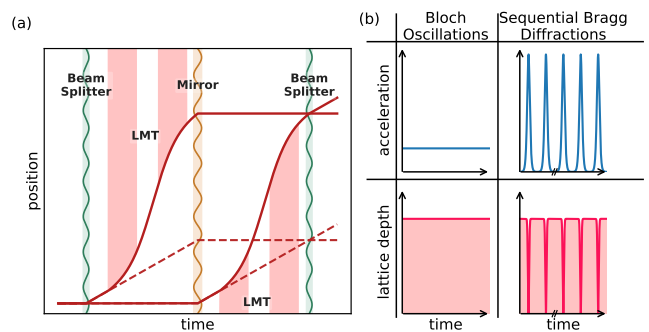


FIG. 1. (a) Space-time diagram of a Large-momentum-Transfer-enhanced Mach-Zehnder atom interferometer. The sequence consists of two beam splitter and a mirror pulse. Each interferometer arm is accelerated and decelerated using LMT sequences in an optical lattice, resulting in a larger momentum separation compared to a standard Mach-Zehnder atom interferometer (dashed lines). (b) Control parameters (acceleration and lattice potential) for Bloch Oscillation and Sequential Bragg Diffraction LMT.

and dark matter [26–32].

In this work, we exploit the temporal periodicity and discrete spatial symmetry of optical lattices within a Floquet framework to extend a recently developed Wannier-Stark model [33] to the full class of elastic LMT scattering methods. Within this unified description, we introduce a parametrized family of Hamiltonians that continuously interpolates between the limiting cases of BOs and SBDs through variation of a single control parameter. This approach exposes the fundamental efficiency and phase-accuracy limits inherent to different

\* These authors contributed equally to this work.

† Currently at ASML Netherlands B.V., De Run 6501, 5504 DR Veldhoven.

‡ Contact author: [klemens.hammerer@uibk.ac.at](mailto:klemens.hammerer@uibk.ac.at)

§ Contact author: [gaaloul@iqo.uni-hannover.de](mailto:gaaloul@iqo.uni-hannover.de)

LMT schemes and enables their direct comparison on equal footing. Furthermore, it identifies previously unexplored operating regimes in which pulse efficiencies can be substantially enhanced, thereby extending the attainable performance beyond that of current state-of-the-art implementations [25].

The paper is structured as follows: We first present the theoretical framework by introducing the general Hamiltonian and presenting a solution of the time-dependent Schrödinger equation based on Floquet theory. We then proceed to parametrize a specific family of Hamiltonians to cover BOs and SBDs as two distinct limits which allows us to evaluate our results by analyzing the efficiency and phase accuracy, drawing comparisons with state-of-the-art experiments. Finally, we present a method for adiabatic preparation of Floquet states in optical lattices and compare our results to exact numerical solutions of the Schrödinger equation.

*Theoretical model*— We consider an atom with a mass  $m$  loaded in an optical lattice which is formed by two counter-propagating beams characterized in the laboratory reference frame by their phases  $\phi_{1,2}$ , their frequencies  $\omega_{1,2}$ , and their opposite wave vectors  $\mathbf{k}_{1,2}$  with  $\mathbf{k}_1 \approx \mathbf{k}_2$ . The phase and frequency differences between these two beams are defined as  $\Delta\phi(t) = \phi_1(t) - \phi_2(t)$  and  $\omega_L(t) = \partial_t(\Delta\phi)$ , respectively. The mean wave vector is given by  $\mathbf{k}_L = (\mathbf{k}_1 - \mathbf{k}_2)/2 = \pi/d$ , where  $d$  is the lattice period. When the two beams overlap, they give rise to a quasi-stationary wave moving with acceleration  $a_L(t) = \dot{\omega}_L(t)/2k_L$  relative to the laboratory reference frame. The laser is detuned far from the frequencies of the internal atomic transitions, allowing for adiabatic elimination of the excited state. This leads to an interaction potential of the form  $V(t) \cos^2(k_L \hat{x} - \Delta\phi(t)/2)$ , with lattice depth  $V(t)$ . In the following we consider time-periodic lattice parameters  $V(t + T_F) = V(t)$  and  $a_L(t + T_F) = a_L(t)$ , where  $T_F$  is the Floquet period. This includes SBDs, where the lattice depth is constant and the lattice acceleration  $a_L(t) = a_0 \sum_n \delta(t - nT_F)$  is a Dirac-comb, as well as BOs, where both lattice depth and acceleration  $a_L(t) = a_0$  are constant. In the following we will relate the Bloch acceleration  $a_0 = 2\hbar k_L/mT_B$  to the Floquet period by setting  $T_B = T_F$ , where  $T_B$  is the Bloch period.

In the co-moving lattice frame [20, 34], the Hamiltonian takes the form

$$H(t) = \frac{\hat{p}^2}{2m} + V(t) \cos^2(k_L \hat{x}) + m a_L(t) \hat{x} \quad (1)$$

with time-periodicity  $H(t + T_F) = H(t)$ . A solution to the time-dependent Schrödinger equation can be obtained by diagonalizing the Floquet operator  $U(T_F)$ , that is, the time-evolution operator over one period [35]. Here, the Floquet operator has a discrete spatial symmetry under translations by  $d$  [36]. This implies that  $U(T_F)$  and the discrete spatial translation operator  $\hat{T}$  share a com-

mon eigenbasis, the Floquet states, defined by

$$U(T_F) |\phi_\alpha(\kappa)\rangle = e^{-i\mathcal{E}_\alpha(\kappa)T_F/\hbar} |\phi_\alpha(\kappa)\rangle, \quad (2)$$

$$\hat{T} |\phi_\alpha(\kappa)\rangle = e^{i\kappa d} |\phi_\alpha(\kappa)\rangle \quad (3)$$

with quasi-momentum  $-k_L \leq \kappa \leq k_L$  and a band index  $\alpha$ . The quasi-energies in general depend on the quasi-momentum  $\kappa$  and are complex numbers of the form  $\mathcal{E}_{\alpha,\ell}(\kappa) = E_\alpha(\kappa) + 2\pi\ell\hbar/T_F - i\Gamma_\alpha(\kappa)/2$  [37]. The imaginary part of the energies represents the linewidth of the Floquet state, determining the tunneling losses to the continuum [33, 37, 38] in the tilted potential of Eq. (1). These losses exist due to the finite size of the system, as in theory the Floquet states are infinitely spread out, which is not possible in a realistic environment. Due to the periodicity of the complex exponential, each quasi-energy corresponds to a set of equivalent representatives given by  $\ell \in \mathbb{Z}$ , where the quantum number  $\ell$  can be associated with the lattice site. The dependence of the quasi-energies  $\mathcal{E}_\alpha(\kappa)$  on the quasi-momentum is discussed in [39]. In the following, we aim to analyze the efficiency of LMT-schemes in terms of their quasi-energies and, in particular, their intrinsic losses quantified by  $\Gamma_\alpha(\kappa)$ .

*Unifying Bloch and sequential Bragg LMT*— To this end, we consider a family of pulses with a constant lattice depth  $V(t) = V_0$ , and an acceleration

$$a_L^{(\eta)}(t) = \frac{1 + \cosh(\eta/2)}{\sinh(\eta/2)} \frac{a_0 \eta e^{-\eta(t/T_F - (n+1/2))}}{(e^{-\eta(t/T_F - (n+1/2))} + 1)^2}, \quad (4)$$

where  $nT_F \leq t < (n+1)T_F$ ,  $a_0 = 2\hbar k_L/mT_F$ . Here,  $\eta \in (0, \infty)$  continuously interpolates between the case of BOs where the acceleration is constant, and SBDs where it converges to a comb of delta-functions. The quasi-momentum  $\kappa$  remains as a degree of freedom of the system, relevant for the LMT efficiency and is fixed via the initial Floquet state. For separate Bragg pulses the quasi-momentum is related to the Bragg resonance condition which is fulfilled at  $\kappa = k_L$ . However for the case of sequential pulses the quasi-momentum can be chosen freely without taking the resonance condition into account. Moreover, we later show that a choice of  $\kappa = 0$  can result in a much higher efficiency of the corresponding LMT sequence. Even though the Bragg resonance condition is in general not fulfilled for a freely chosen quasi-momentum, we will here call the entire regime of sequential delta-like acceleration pulses ‘SBD’.

Fig. 2(a) illustrates the smooth interpolation between BOs and SBDs characterized by the linewidth  $\Gamma_0$  of the Floquet state  $|\phi_0(\kappa=0)\rangle$  of the fundamental band  $\alpha = 0$ . In general, the linewidth  $\Gamma_\alpha$  corresponds to the tunneling loss rate of the  $\alpha$ -th Floquet state to the continuum, either directly or via intermediate Floquet states. In the BO regime, the spectrum resembles those previously reported in [33], where the peaks in the tunneling loss rate can be explained via tunneling resonances

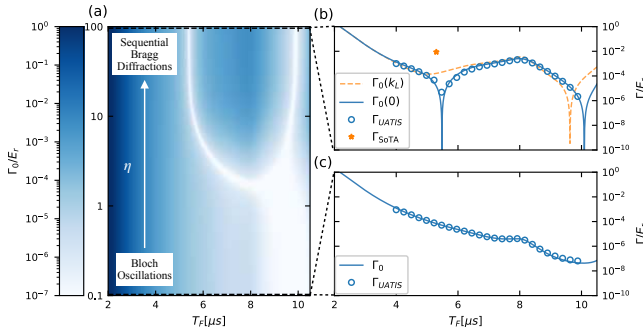


FIG. 2. (a) Density map of the tunneling loss rate  $\Gamma_0$  of the Floquet-groundstate at quasi-momentum  $\kappa = 0$   $|\phi_0(\kappa = 0)\rangle$  versus Floquet period  $T_F$  and interpolation parameter  $\eta$  (cf. (4)) for a lattice depth of  $V_0 = 50E_r$ . The color bar is cut off at  $10^{-7}$  to increase the contrast. (b) Cut through the density map (a) in SBD limit at  $\eta = 100$  (solid blue line) corresponding to  $\kappa = 0$ , results of exact numerical simulations (blue points), tunneling loss rate in SBDs limit for  $\kappa = k_L$  (orange line) and overall loss rate of state-of-the-art experiment [25] (orange star). The experimental loss rate deviates from its fundamental limit at  $\kappa = k_L$  due pulse-to-pulse fluctuations and spontaneous emission losses. (c) Cut through the density map (a) in BO limit at  $\eta = 0.1$  (solid blue line) and results of exact numerical simulations (blue points). The exact numerical simulations are performed with the 'Universal Atom Interferometer Simulator' (UATIS) [40].

between different Wannier-Stark ladders [33]. Remarkably, beyond a certain threshold for  $\eta$ , one observes sharp *anti-resonances* in the line width  $\Gamma_0$ , corresponding to a pronounced suppression of tunneling losses. This phenomenon is reminiscent of coherent suppression of tunneling [41] and dynamical localization in shaken optical lattices [42–46], which also occurs for excited bands [47]. Figs. 2(b, c) show two representative cuts through the density map Fig. 2(a), obtained by fixing the parameter  $\eta$  to values corresponding to the BO and SBD regimes, respectively. At anti-resonances the SBD regime shows a clear enhancement in fundamental efficiency compared to the BO case for the same periods  $T_F$ , thus allowing for highly efficient LMT at fast transfer rates.

Fig. 2(b) highlights the importance of the quasi-momentum, by showing the clear improvement from  $\kappa = k_L$  to  $\kappa = 0$  at small Floquet periods. Even though  $\kappa = k_L$  might be the more intuitive choice as it fulfills the Bragg resonance condition for single pulses, the first anti-resonance is located at almost twice the Floquet period as for  $\kappa = 0$ . Therefore reaching the same efficiency would correspond to almost half the momentum transfer rate. Additionally, spontaneous emission losses have to be considered. To access the fundamental efficiency enhancements due to the anti-resonances, a certain amount of laser power is required [48].

This enhancement in pulse efficiency could be exploited in gravity gradiometry among other applications. With

a 20W laser power and a beam waist  $w = 1.6$  mm at the above-mentioned resonance minima of the SBD pulse train at  $T_F = 5.5\ \mu\text{s}$  and  $\kappa = 0$ , one could efficiently realize pulse sequences of  $1000\ \hbar k_L$  for a baseline of 100 m. We could anticipate a single-shot gravity gradient sensitivity up to  $10^{-6}\text{E}$  ( $1\text{E} = 10^{-9}\ \text{s}^{-2}$ ). Ultimately, this could be pushed further in folded geometries with more momentum transfer reaching sensitivities required for Gravitational Wave detection, dark matter/energy searches or post-Newtonian effect measurements.

*Phase Uncertainty*— One of the main contributors to the overall phase uncertainty is induced by intensity asymmetries of the lattice between the interferometer arms and noise that could couple to them. The phase imprinted by a single LMT pulse of  $2\hbar k_L$  is given by  $\phi_\alpha = E_\alpha T_F/\hbar$  [49] for  $\ell = 0$ . A lattice depth difference  $\Delta V$  between the arms will therefore cause a phase shift of

$$\frac{\Delta\phi_\alpha}{N\frac{\Delta V}{V_0}} = 2\pi \left| \frac{\partial E_\alpha}{\partial V_0} \right| \frac{V_0}{ma_L d}. \quad (5)$$

We normalize the phase shift to the number of Floquet periods  $N$  and the relative lattice depth difference  $\Delta V/V_0$ . Note, that Eq. (5) also covers dephasing caused by pulse-to-pulse intensity fluctuations within one interferometer arm. In Fig. 3(a,b) we show these phase changes for an exemplary Floquet period in the limit of BOs and of SBDs, respectively. As Fig. 3 demonstrates, there is no difference between the phase uncertainty induced by BOs and SBDs and therefore the energies  $E_{\alpha,\ell}$  only depend on the average acceleration, but not its temporal profile.

There are particular lattice depths where the phase uncertainty  $\Delta\phi_\alpha$  is zero for some excited states. At these parameters, the system is robust to dephasing caused by noisy lattice depth differences. Note that for the case of BOs this corresponds to the phenomenon of "magic" lattice depths reported in [50]. However, the increased tunneling loss rate  $\Gamma_\alpha$  of excited Floquet bands, does not allow for reaching high-fidelity Bloch LMT pulses robust to dephasing. The existence of these subsystems robust to the dephasing of Eq. (5) in the general case opens the room for optimization, where high-fidelity pulses can also be realized for excited states [47]. Combining high-efficiency LMT pulses with robustness to dephasing would be promising for high-sensitivity measurements.

*Adiabatic Preparation*—To validate our theoretical framework, we perform numerical simulations using the 'Universal Atom Interferometer Simulator' (UATIS) [40]. First, we define an adiabatic preparation sequence, as demonstrated in Fig. 4. This preparation method represents a different, straightforward approach compared to the optimal control discussed in [25]. Next, we quantify the losses to the continuum by computing the decayed fraction of the Floquet states after a LMT sequence (c.f.

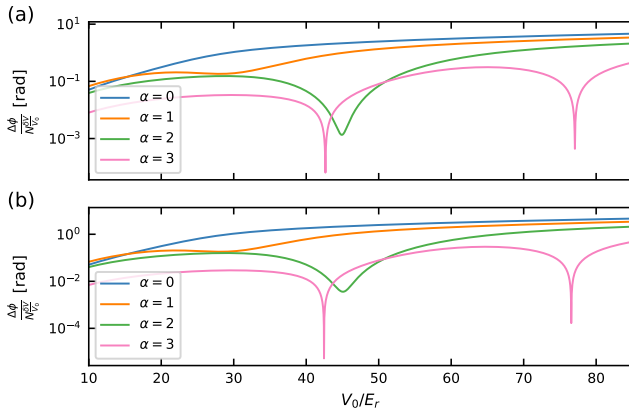


FIG. 3. Phase uncertainty induced by lattice depth differences versus lattice depth  $V_0$  for a Floquet period of  $T_F = 5.3\mu\text{s}$ . The specific Floquet period was chosen to cover the experiment [25] at a lattice depth of  $V_0 = 50E_r$  in the limit of SBDs. The phase uncertainty is determined for the first five Floquet bands in the limit of BOs  $\eta = 0.1$  (a) and the limit of SBDs  $\eta = 100$  (b). The average AC Stark shift is suppressed here.

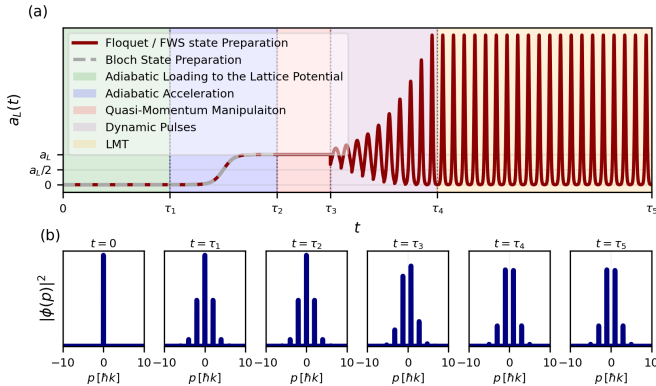


FIG. 4. (a) Schematic illustration of lattice acceleration in arbitrary units versus time  $t$  for adiabatic preparation of Floquet state  $|\phi_0(\kappa)\rangle$  and SBDs LMT pulse. The pulse sequence is split into distinct steps:  $t \in [0, \tau_1]$  adiabatic ramping of lattice potential;  $t \in (\tau_1, \tau_2]$  adiabatic ramping of lattice acceleration;  $t \in (\tau_2, \tau_3]$  BOs controlling the quasi-momentum  $\kappa$ ;  $t \in (\tau_3, \tau_4]$  adiabatic change of lattice acceleration function  $\eta$ ;  $t \in (\tau_4, \tau_5]$  SBDs LMT pulse. Note that the first two steps correspond to adiabatic Bloch state preparation [51]. (b) Momentum representation probability amplitude of wavefunction in arbitrary units at time-steps  $t = 0, \tau_1, \tau_2, \tau_3, \tau_4, \tau_5$  in the co-moving lattice frame.

Fig. 2(b,c)). Furthermore, we calculate the phase uncertainty by simulating two LMT sequences corresponding to the two arms of the interferometer. In one arm, the state evolves under the standard LMT sequence with an unperturbed lattice potential  $V_0$ , while for the other arm, a fluctuation  $\Delta V$  is introduced to the LMT sequence. Finally, we obtain the dephasing from the relative phase accumulated between the two states, which match the results shown in Fig. 3.

*Conclusion*— We have developed a unified theoretical framework for large-momentum-transfer methods in optical lattices based on a Floquet description of elastic light–atom scattering. Within this framework, we introduced a continuous parametrization that encompasses Bloch oscillations and sequential Bragg diffraction as limiting cases, enabling a direct and quantitative comparison of their efficiency and phase properties. We further proposed an adiabatic preparation scheme for Floquet states that provides controlled access to the relevant scattering regimes. The validity of our approach is established through quantitative agreement with exact numerical solutions of the Schrödinger equation as well as with recent state-of-the-art experimental results. Beyond reproducing existing implementations, the framework identifies clear pathways for further optimization, including the realization of higher-efficiency pulses at shorter durations and the development of schemes that are more robust against dephasing. Such optimizations can be systematically explored both within the parameter space considered here and through alternative parametrizations of the underlying Hamiltonian. Taken together, the fundamental efficiency limits identified for experimentally relevant parameters and the demonstrated flexibility of the Floquet approach provide a solid foundation for the design of next-generation high-precision atom-interferometric experiments.

*Acknowledgement*— We thank Ernst Rasel, Pierre Cladé, and David Weld for fruitful discussions. A.A and P.M would like to express his gratitude to their colleagues in T-SQUAD and LCAR for their feedback and support. This work was funded by the Deutsche Forschungsgemeinschaft (German Research Foundation) under Germany’s Excellence Strategy (EXC-2123 QuantumFrontiers Grant No. 390837967) and through CRC 1227 (DQ-mat) within project No. A05. We also acknowledge funding by the by the AGAPES project – grant No. 530096754 within the ANR-DFG 2023 Programme.

---

- [1] R. Geiger, A. Landragin, S. Merlet, and F. Pereira Dos Santos, [AVS Quantum Science](#) **2**, 024702 (2020).
- [2] R. Geiger, V. Ménoret, G. Stern, N. Zahzam, P. Cheinet, B. Battelier, A. Villing, F. Moron, M. Lours, Y. Bidel, A. Bresson, A. Landragin, and P. Bouyer, [Nature Communications](#) **2**, 474 (2011).
- [3] P. Cheiney, L. Fouché, S. Templier, F. Napolitano, B. Battelier, P. Bouyer, and B. Barrett, [Phys. Rev. Appl.](#) **10**, 034030 (2018).
- [4] M. Kasevich and S. Chu, [Phys. Rev. Lett.](#) **67**, 181 (1991).
- [5] M. Kasevich and S. Chu, [Applied Physics B](#) **54**, 321 (1992).
- [6] J. B. Fixler, G. T. Foster, J. M. McGuirk, and M. A. Kasevich, [Science](#) **315**, 74 (2007), <https://www.science.org/doi/pdf/10.1126/science.1135459>.

[7] K. Bongs, M. Holynski, J. Vovrosh, P. Bouyer, G. Condon, E. Rasel, C. Schubert, W. P. Schleich, and A. Roura, *Nature Reviews Physics* **1**, 731 (2019).

[8] G. Lamporesi, A. Bertoldi, L. Cacciapuoti, M. Prevedelli, and G. M. Tino, *Phys. Rev. Lett.* **100**, 050801 (2008).

[9] R. H. Parker, C. Yu, W. Zhong, B. Estey, and H. Müller, *Science* **360**, 191 (2018), <https://www.science.org/doi/pdf/10.1126/science.aap7706>.

[10] L. Morel, Z. Yao, P. Cladé, and S. Guellati-Khélifa, *Nature* **588**, 61 (2020).

[11] S. Dimopoulos, P. W. Graham, J. M. Hogan, and M. A. Kasevich, *Phys. Rev. D* **78**, 042003 (2008).

[12] P. Asenbaum, C. Overstreet, M. Kim, J. Curti, and M. A. Kasevich, *Phys. Rev. Lett.* **125**, 191101 (2020).

[13] J. M. McGuirk, M. J. Snadden, and M. A. Kasevich, *Phys. Rev. Lett.* **85**, 4498 (2000).

[14] H. Müller, S.-w. Chiow, Q. Long, S. Herrmann, and S. Chu, *Phys. Rev. Lett.* **100**, 180405 (2008).

[15] S.-w. Chiow, T. Kovachy, H.-C. Chien, and M. A. Kasevich, *Phys. Rev. Lett.* **107**, 130403 (2011).

[16] B. Plotkin-Swing, D. Gochnauer, K. E. McAlpine, E. S. Cooper, A. O. Jamison, and S. Gupta, *Phys. Rev. Lett.* **121**, 133201 (2018).

[17] T. Wilkason, M. Nantel, J. Rudolph, Y. Jiang, B. E. Garber, H. Swan, S. P. Carman, M. Abe, and J. M. Hogan, *Phys. Rev. Lett.* **129**, 183202 (2022).

[18] K. Kotru, D. L. Butts, J. M. Kinast, and R. E. Stoner, *Phys. Rev. Lett.* **115**, 103001 (2015).

[19] T. Lévéque, A. Gauguet, F. Michaud, F. Pereira Dos Santos, and A. Landragin, *Phys. Rev. Lett.* **103**, 080405 (2009).

[20] E. Peik, M. Ben Dahan, I. Bouchoule, Y. Castin, and C. Salomon, *Phys. Rev. A* **55**, 2989 (1997).

[21] H. Müller, S.-w. Chiow, S. Herrmann, and S. Chu, *Phys. Rev. Lett.* **102**, 240403 (2009).

[22] P. Cladé, S. Guellati-Khélifa, F. m. c. Nez, and F. m. c. Biraben, *Phys. Rev. Lett.* **102**, 240402 (2009).

[23] M. Gebbe, J.-N. Siemß, M. Gersemann, H. Müntinga, S. Herrmann, C. Lämmerzahl, H. Ahlers, N. Gaaloul, C. Schubert, K. Hammerer, S. Abend, and E. M. Rasel, *Nature Communications* **12**, 2544 (2021).

[24] A. Béguin, T. Rodzinka, L. Calmels, B. Allard, and A. Gauguet, *Phys. Rev. Lett.* **131**, 143401 (2023).

[25] T. Rodzinka, E. Dionis, L. Calmels, S. Beldjoudi, A. Béguin, D. Guéry-Odelin, B. Allard, D. Sugny, and A. Gauguet, *Nature Communications* **15**, 10281 (2024).

[26] P. W. Graham, J. M. Hogan, M. A. Kasevich, and S. Rajendran, *Phys. Rev. Lett.* **110**, 171102 (2013).

[27] B. Canuel, A. Bertoldi, L. Amand, E. Pozzo di Borgo, T. Chantrait, C. Danquigny, M. Dovale Álvarez, B. Fang, A. Freise, R. Geiger, J. Gillot, S. Henry, J. Hinderer, D. Holleville, J. Junca, G. Lefèvre, M. Merzougui, N. Mielec, T. Monfret, S. Pelisson, *et al.*, *Scientific Reports* **8**, 14064 (2018).

[28] B. Canuel, S. Abend, P. Amaro-Seoane, F. Badaracco, Q. Beaufils, A. Bertoldi, K. Bongs, P. Bouyer, C. Braxmaier, W. Chaibi, N. Christensen, F. Fitzek, G. Flouris, N. Gaaloul, S. Gaffet, C. L. Garrido Alzar, R. Geiger, S. Guellati-Khélifa, K. Hammerer, *et al.*, *Classical and Quantum Gravity* **37**, 225017 (2020).

[29] M.-S. Zhan, J. Wang, W.-T. Ni, D.-F. Gao, G. Wang, L.-X. He, R.-B. Li, L. Zhou, X. Chen, J.-Q. Zhong, B. Tang, Z.-W. Yao, L. Zhu, Z.-Y. Xiong, S.-B. Lu, G.-H. Yu, Q.-F. Cheng, M. Liu, Y.-R. Liang, P. Xu, *et al.*, *International Journal of Modern Physics D* **29**, 1940005 (2020), <https://doi.org/10.1142/S0218271819400054>.

[30] M. Abe, P. Adamson, M. Borcean, D. Bortoletto, K. Bridges, S. P. Carman, S. Chattopadhyay, J. Coleman, N. M. Curfman, K. DeRose, T. Deshpande, S. Dimopoulos, C. J. Foot, J. C. Frisch, B. E. Garber, S. Geer, V. Gibson, J. Glick, P. W. Graham, S. R. Hahn, *et al.*, *Quantum Science and Technology* **6**, 044003 (2021).

[31] L. Badurina, E. Bentine, D. Blas, K. Bongs, D. Bortoletto, T. Bowcock, K. Bridges, W. Bowden, O. Buchmueller, C. Burrage, J. Coleman, G. Elertas, J. Ellis, C. Foot, V. Gibson, M. Haehnelt, T. Harte, S. Hedges, R. Hobson, M. Holynski, T. Jones, *et al.*, *Journal of Cosmology and Astroparticle Physics* **2020** (05), 011.

[32] A. Abdalla, M. Abe, S. Abend, M. Abidi, M. Aidelsburger, A. Alibabaei, B. Allard, J. Antoniadis, G. Arduini, N. Augst, P. Balamatsias, A. Balaž, H. Banks, R. L. Barcklay, M. Barone, M. Barsanti, M. G. Bason, A. Bassi, J.-B. Bayle, C. F. A. Baynham, *et al.*, *EPJ Quantum Technology* **12**, 42 (2025).

[33] F. Fitzek, J.-N. Kirsten-Siemß, E. M. Rasel, N. Gaaloul, and K. Hammerer, *Phys. Rev. Res.* **6**, L032028 (2024).

[34] See Supplemental Material Section I. for detailed unitary frame transformations.

[35] M. Holthaus, *Journal of Physics B: Atomic, Molecular and Optical Physics* **49**, 013001 (2015).

[36] See Supplemental Material Section II.A. for detailed calculation of spatial symmetry.

[37] G. Nenciu, *Rev. Mod. Phys.* **63**, 91 (1991).

[38] G. H. Wannier, *Phys. Rev.* **117**, 432 (1960).

[39] See Supplemental Material Section II.B for detailed discussion of quasi-momentum dependency.

[40] F. Fitzek, J.-N. Siemß, S. Seckmeyer, H. Ahlers, E. M. Rasel, K. Hammerer, and N. Gaaloul, *Scientific Reports* **10**, 22120 (2020).

[41] F. Grossmann, T. Dittrich, P. Jung, and P. Hänggi, *Phys. Rev. Lett.* **67**, 516 (1991).

[42] A. Eckardt, M. Holthaus, H. Lignier, A. Zenesini, D. Ciampini, O. Morsch, and E. Arimondo, *Phys. Rev. A* **79**, 013611 (2009).

[43] K. Yashima, K.-i. Hino, and N. Toshima, *Phys. Rev. B* **68**, 235325 (2003).

[44] H. Lignier, C. Sias, D. Ciampini, Y. Singh, A. Zenesini, O. Morsch, and E. Arimondo, *Phys. Rev. Lett.* **99**, 220403 (2007).

[45] T. Shimasaki, Y. Bai, H. E. Kondakci, P. Dotti, J. E. Pagett, A. R. Dardia, M. Prichard, A. Eckardt, and D. M. Weld, *Phys. Rev. Lett.* **133**, 083405 (2024).

[46] T. Shimasaki, M. Prichard, H. E. Kondakci, J. E. Pagett, Y. Bai, P. Dotti, A. Cao, A. R. Dardia, T.-C. Lu, T. Grover, and D. M. Weld, *Nature Physics* **20**, 409 (2024).

[47] See Supplemental Material Section IV. Fig. S3(b).

[48] See Supplemental Material Section III. for spontaneous emission model.

[49] See Supplemental Material Section II.A. for time-evolution of Floquet states.

[50] K. E. McAlpine, D. Gochnauer, and S. Gupta, *Phys. Rev. A* **101**, 023614 (2020).

[51] J.-N. Siemß, F. Fitzek, S. Abend, E. M. Rasel, N. Gaaloul, and K. Hammerer, *Phys. Rev. A* **102**, 033709 (2020).

# Supplemental Material: Fundamental Limits of Large Momentum Transfer in Optical Lattices

Ashkan Alibabaei,<sup>1,\*</sup> Patrik Mönkeberg,<sup>2,\*</sup> Florian Fitzek,<sup>1,2,†</sup> Alexandre Gauguet,<sup>3</sup> Baptiste Allard,<sup>3</sup> Klemens Hammerer,<sup>2,4,5,‡</sup> and Naceur Gaaloul<sup>1,§</sup>

<sup>1</sup>*Institute of Quantum Optic, Leibniz University of Hannover, Welfengarten 1 30167 Hannover, Germany*  
<sup>2</sup>*Institute of Theoretical Physics, Leibniz University of Hannover, Appelstrasse 2 30167 Hannover, Germany*

<sup>3</sup>*Laboratoire Collisions Agrégats Réactivité, FERMI, Université de Toulouse  
and CNRS UMR5589, 118 Route de Narbonne, F-31062 Toulouse, France*

<sup>4</sup>*Institute for Theoretical Physics, University of Innsbruck, 6020 Innsbruck, Austria*

<sup>5</sup>*Institute for Quantum Optics and Quantum Information of the Austrian Academy of Sciences, 6020 Innsbruck, Austria*  
(Dated: February 3, 2026)

## CONTENTS

I. Hamiltonian and lattice parameters	1
A. Laboratory frame	1
B. Reduced Lattice Frame	2
C. Lattice Frame	2
II. Floquet solution	3
A. Floquet basis	3
B. Quasi-momentum	3
III. Spontaneous emission losses	4
IV. Numerical methods	5
A. Diagonalization of Floquet operator	5
B. Quasi-energy sorting	6
References	7

## I. HAMILTONIAN AND LATTICE PARAMETERS

In this section, we present an overview over the Hamiltonian and control parameters in three different reference frames and list their properties. Each of the presented reference frames is relevant for different parts of the discussion or calculations of the model presented in the main article.

### A. Laboratory frame

In the laboratory frame the Hamiltonian has the following form

$$H_{\text{lab}}(t) = \frac{\hat{p}^2}{2m} + V(t) \cos^2[k_L(\hat{x} - x_L(t))] \quad (\text{S1})$$

with a periodically modulated lattice depth

$$V(t) = V(t + T_F) \quad (\text{S2})$$

\* These authors contributed equally to this work.

† Currently at ASML Netherlands B.V., De Run 6501, 5504 DR Veldhoven.

‡ Contact author: [klemens.hammerer@uibk.ac.at](mailto:klemens.hammerer@uibk.ac.at)

§ Contact author: [gaaloul@iqo.uni-hannover.de](mailto:gaaloul@iqo.uni-hannover.de)

and a lattice position  $x_L(t)$  corresponding to a periodically modulated acceleration

$$\begin{aligned} x_L(t) &= \int_0^t dt' \int_0^{t'} dt'' a_L(t''), \\ p_L(t) &= \int_0^t dt' m a_L(t'), \\ a_L(t) &= a_L(t + T_F). \end{aligned} \tag{S3}$$

Note that the lattice depth is given by the effective two-photon Rabi frequency  $\Omega(t)$  via  $V(t) = 2\hbar\Omega(t)$ . Additionally we define the acceleration averaged over one period as

$$\bar{a}_L := \frac{1}{T_F} \int_{t_0}^{t_0+T_F} dt a_L(t), \tag{S4}$$

### B. Reduced Lattice Frame

The reduced lattice frame is defined as a co-moving reference frame where the momentum is still measured with respect to the laboratory frame. The Hamiltonian takes the form

$$H_{\text{rlf}}(t) = \frac{(\hat{p} - p_L(t))^2}{2m} + V(t) \cos^2(k\hat{x}). \tag{S5}$$

We used  $H_{\text{rlf}}(t) = U(t)H_{\text{lab}}U^\dagger(t) + i\hbar\dot{U}U^\dagger(t)$  and

$$U(t) = \exp(i\hat{p}x_L(t)/\hbar + i\gamma_U(t)/\hbar), \tag{S6}$$

where  $\gamma_U(t) = p_L(t)^2/2m$ . We used the identities

$$e^{\hat{X}} \hat{Y} e^{-\hat{X}} = \sum_{n=0}^{\infty} \frac{[\hat{X}, \hat{Y}]_m}{m!} = \hat{Y} + [\hat{X}, \hat{Y}] + \frac{1}{2!} [\hat{X}, [\hat{X}, \hat{Y}]] + \dots, \tag{S7}$$

$$\frac{d}{dt} e^{\hat{X}(t)} = e^{\hat{X}(t)} \int_0^1 d\lambda e^{-\lambda\hat{X}(t)} \left( \frac{d}{dt} \hat{X}(t) \right) e^{\lambda\hat{X}(t)}. \tag{S8}$$

Note that the Hamiltonian in the reduced lattice frame  $H_{\text{rlf}}(t)$  has a discrete translation invariance with period  $d = \pi/k_L$ , that is

$$\hat{T} H_{\text{rlf}}(t) \hat{T}^\dagger = H_{\text{rlf}}(t), \tag{S9}$$

where

$$\hat{T} = e^{i\hat{p}d/\hbar} \tag{S10}$$

is the discrete spatial translation operator, shifting by distance  $d$ .

### C. Lattice Frame

Finally in the lattice frame, which is co-moving in position and momentum, the Hamiltonian is

$$H_{\text{lat}}(t) = \frac{\hat{p}^2}{2m} + V(t) \cos(2k\hat{z}) + m a_L(t) \hat{z} \tag{S11}$$

where we used  $H_{\text{lat}}(t) = \tilde{U}(t)H_{\text{rlf}}(t)\tilde{U}^\dagger(t) + i\hbar\dot{\tilde{U}}(t)\tilde{U}^\dagger(t)$  with

$$\tilde{U}(t) = \exp(-i\hat{x}p_L(t)/\hbar). \tag{S12}$$

The Hamiltonian in the lattice frame is time-periodic but *not* translation invariant

$$H_{\text{lat}}(t + T_F) = H_{\text{lat}}(t), \quad \hat{T} H_{\text{lat}}(t) \hat{T}^\dagger = H_{\text{lat}}(t) + m a_L(t) d. \tag{S13}$$

Note that the general Hamiltonian (S11) covers both Bloch Oscillations (BOs) and Sequential Bragg Diffractions (SBDs). For BOs we have a constant acceleration  $a_L(t) \equiv a_0$  and a constant lattice depth  $V(t) \equiv V_0$ , while for SBDs we have a  $\delta$ -comb acceleration  $a_L(t) = a_0 \sum_n \delta(t - nT_F)$  and a constant lattice depth.

## II. FLOQUET SOLUTION

The time-periodicity of the Hamiltonian in the lattice frame (S13) enables us to find the eigenstates and eigenenergies of the system via Floquet theory.

### A. Floquet basis

Despite the fact that  $H_{\text{lat}}(t)$  has no spatial periodicity (S13), the **Floquet operator**  $U_{\text{lat}}(t_0 + T_F, t_0)$  is invariant under discrete translations by  $d$ , provided the momentum  $\Delta p_L = p_L(t_0 + T_F) - p_L(t_0)$  imparted per period is a multiple of  $2\hbar k_L$ . We show this by expressing the time evolution operator in the lattice frame as

$$U_{\text{lat}}(t, t_0) = \tilde{U}(t)U_{\text{rlf}}(t, t_0)\tilde{U}^\dagger(t_0), \quad (\text{S14})$$

where  $\tilde{U}(t)$  is the unitary given in (S12) and  $U_{\text{rlf}}(t, t_0)$  is the time evolution operator in the reduced lattice frame. The latter is spatially periodic  $\hat{T}U_{\text{rlf}}(t, t_0)\hat{T}^\dagger = U_{\text{rlf}}(t, t_0)$  due to the spatial periodicity of the Hamiltonian in the reduced lattice frame (S9). In the lattice frame we then have

$$\hat{T}U_{\text{lat}}(t, t_0)\hat{T}^\dagger = e^{-id(p_L(t) - p_L(t_0))/\hbar}U_{\text{lat}}(t, t_0), \quad (\text{S15})$$

and for the Floquet operator we can conclude

$$\hat{T}U_{\text{lat}}(t_0 + T, t_0)\hat{T}^\dagger = e^{-id\Delta p_L/\hbar}U_{\text{lat}}(t_0 + T, t_0). \quad (\text{S16})$$

Thus, spatial periodicity requires  $d\Delta p_L/\hbar = 2\pi n$ , which according to (S4) and  $d = \pi/k_L$  is equivalent to

$$\bar{a}_L = \frac{2n\hbar k_L}{mT_F}. \quad (\text{S17})$$

Under condition (S17) we thus have for all  $t_0$

$$[\hat{T}, U_{\text{lat}}(t_0 + T_F, t_0)] = 0. \quad (\text{S18})$$

Note, that for the special case of BOs without an externally imposed time period  $T_F$ , the condition (S17) sets the connection between the constant acceleration  $a_L \equiv a_0$  and the period. The case  $n = 1$  sets the shortest period, the Bloch period  $T_B = 2\hbar k_L/ma_0$ . For any other pulse sequence, with a chosen acceleration  $a_L(t)$  and period  $T_F$ , the condition (S17) determines the number  $n$  of momentum quanta  $2\hbar k_L$  imparted per period. If we define the equivalent Bloch period for a given average acceleration  $\bar{a}_L$  via  $T_B = 2\hbar k_L/m\bar{a}_L$ , then  $n = T_F/T_B$  gives the ratio of the external time period to the equivalent Bloch period. This allows us to directly compare the case of BOs to any other case with constant lattice depth.

The fact that the Floquet operator is invariant under discrete translations (S18) implies that there exists a basis of common eigenstates, the Floquet states

$$U_{\text{lat}}(t_0 + T_F, t_0)|\phi_\alpha(\kappa, t_0)\rangle = e^{-i\mathcal{E}_\alpha(\kappa, t_0)T_F/\hbar}|\phi_\alpha(\kappa, t_0)\rangle \quad (\text{S19})$$

$$\hat{T}|\phi_\alpha(\kappa, t_0)\rangle = e^{i\kappa d}|\phi_\alpha(\kappa, t_0)\rangle \quad (\text{S20})$$

with quasi-momentum  $-k \leq \kappa \leq k$  and a band index  $\alpha$  [1]. Due to the discrete spatial invariance of the Floquet operator (cf. (S18)), the quantum number  $\ell$  obtained from reconstructing the modulo  $2\pi$  invariance of the quasi-energies can be identified with the lattice site.

The time-evolved Floquet states are defined as

$$|\Phi_\alpha(\kappa_0, t)\rangle := e^{i\mathcal{E}_{\alpha, \ell}(\kappa)(t-t_0)/\hbar}U_{\text{lat}}(t, t_0)|\phi_\alpha(\kappa_0, t_0)\rangle \quad (\text{S21})$$

where the dynamical phase  $e^{i\mathcal{E}_{\alpha, \ell}(\kappa)(t-t_0)/\hbar}$  fixes to the *U(1) gauge freedom* of the Floquet states and ensures that the Floquet states are periodic in time.

### B. Quasi-momentum

In the general case, the Floquet states as well as the quasi-energy spectrum depend on the quasi-momentum  $\kappa$ . Note, that in the case of constant acceleration and lattice depth, i.e. for BOs, it can be shown that the spectrum is independent of the

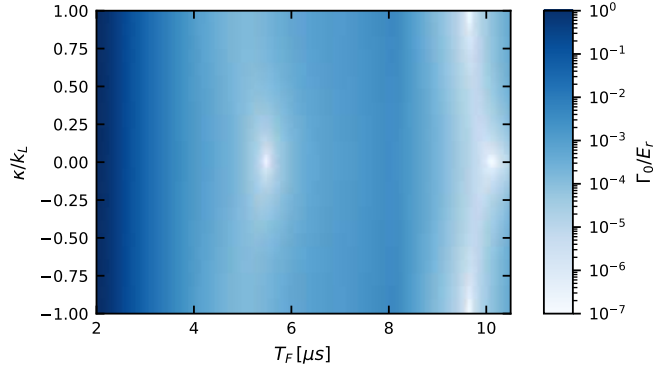


FIG. S1. Tunneling loss rate  $\Gamma_0$  of Floquet groundstate in the limit of SBDs ( $\eta = 100$ ) versus Floquet period  $T_F$  and quasi-momentum  $\kappa$  for a lattice depth  $V_0 = 50E_r$ . The colorbar is cut off at  $10^{-7}$  to increase contrast.

quasi-momentum and a subsequent basis change to Wannier-Stark states, which are also independent of  $\kappa$ , can be performed [2]. However, since the quasi-momentum  $\kappa$  in general remains a relevant quantum number, we will solely use the Floquet basis here.

Therefore for a given lattice depth  $V_0$  and Floquet period  $T_F$ , two degrees of freedom remain: (i) the acceleration type that determines the LMT method, i.e.  $\eta$  in the parametrization which we presented in the main text, and (ii) the quasi-momentum  $\kappa$  which is determined by the relative momentum between the atoms and the lattice. For an atomic cloud with a given temperature, multiple quasi-momentum states will contribute to the overall LMT sequence. Due to the periodic behavior of both the quasi-energy spectrum and the Floquet states with the quasi-momentum, it suffices to explore only the first Brillouin zone, i.e.  $\kappa \in [-k_L, k_L]$ , to find the optimal quasi-momentum to perform LMT sequences at for given lattice parameters.

Fig. S1 shows the quasi-momentum dependency across one Brillouin zone of the tunneling loss rate of the fundamental Floquet band  $\Gamma_0(\kappa)$  for different Floquet periods. This covers both cases studied in the main text, namely  $\kappa = 0$  and  $\kappa = k_L$ , where the latter is experimentally explored by Rodzinka et al. [3]. Fig. S1 especially shows that for the assumed lattice depth of  $V_0 = 50E_r$ ,  $\kappa = 0$  is the optimal choice for efficient LMT at high transfer rates in the SBDs regime. Additionally, the anti-resonances have a finite width in  $\kappa$ , which allows for utilization of the corresponding efficiency enhancement even for finite-temperature initial atomic clouds, given that the temperature is below a certain threshold.

Due to the deep lattice depths we consider here, the real Floquet bands  $E_\alpha(\kappa)$  are flat, more precisely the relative band width is on the order of  $\Delta E_\alpha/E_\alpha \sim 10^{-5} - 10^{-7}$  for the parameter regimes we consider here.

### III. SPONTANEOUS EMISSION LOSSES

In this section, we estimate the spontaneous emission losses for LMT pulses that use a constant lattice depth, therefore including the parametrization presented in the main text and thus BOs and SBDs. To simplify the analysis, we consider all atoms that undergo a spontaneous scattering event as lost and therefore only reducing the overall number of atoms. In general these atoms can undergo transitions to different Floquet bands due to the spontaneous scattering event, resulting in more complex dynamics. However, for sufficiently small spontaneous emission losses, these effects can be effectively suppressed. We estimate the spontaneous scattering rate using [4] as

$$\hbar\Gamma_{\text{sp}} = \frac{\Gamma_{\text{nat}}}{|\Delta|} \langle V(\hat{x}) \rangle, \quad (\text{S22})$$

where  $\Gamma_{\text{nat}}$  is the natural linewidth of the relevant atomic transition,  $\Delta$  is the detuning and  $\langle \cdot \rangle$  denotes the average with respect to the atomic state. Since we only consider deep lattices in this work, we can apply the harmonic approximation to the average potential of a blue detuned lattice

$$\hbar\Gamma_{\text{sp}} = \frac{\Gamma_{\text{nat}}}{|\Delta|} \frac{\sqrt{V_0 E_r}}{2}. \quad (\text{S23})$$

Next, we relate the lattice depth  $V_0$  to the power  $P$  and waist  $w$  of a Gaussian laser beam via

$$V_0 = \frac{3\pi c^2}{2\omega_0^2} \frac{\Gamma_{\text{nat}}}{|\Delta|} \frac{2P}{\pi w^2}, \quad (\text{S24})$$

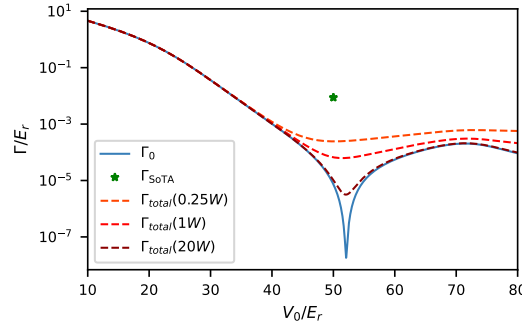


FIG. S2. Tunneling loss rate and total loss rate considering fundamental tunneling losses and spontaneous emission losses for a Floquet period  $T_F = 5.3 \mu\text{s}$  versus lattice depth  $V_0$ . The spontaneous emission losses are estimated in the presented naive model via (S25) for three different laser powers  $P = 250 \text{ mW}, 1 \text{ W}, 20 \text{ W}$  and a fixed beam waist of  $w = 1.6 \text{ mm}$ . Additionally, the green point shows the loss rate reported in [3] for comparision.

where  $\omega_0$  denotes the atomic resonance frequency and  $c$  the speed of light. Inserting this into Eq. (S23) results in

$$\hbar\Gamma_{\text{sp}} = \frac{\omega_0^3 w^2}{6c^2 P} \sqrt{V_0^3 E_r} = \frac{2\omega_0^3}{3\pi c^2} \frac{\sqrt{V_0^3 E_r}}{2I_0}, \quad (\text{S25})$$

where  $I_0 = 2P/\pi w^2$  is the intensity. The spontaneous emission losses can be calculated via

$$1 - P_{\text{sp}} = 1 - e^{-\Gamma_{\text{sp}}\tau}, \quad (\text{S26})$$

where  $\tau$  is the total time of the LMT sequence. In Fig. S2 we compare the tunneling losses, presented in the main article, and the spontaneous emission losses estimated via Eqs. (S25) and (S26). We assume a beam waist of  $w = 1.6 \text{ mm}$  here, as well as for the power numbers given in the main text.

#### IV. NUMERICAL METHODS

##### A. Diagonalization of Floquet operator

We now present a numerical routine to calculate the Floquet states and the complex spectrum. We work in the plane-wave momentum basis  $|2n\hbar k_L + \hbar\kappa\rangle$  with  $n \in \mathbb{Z}$  and quasi-momentum  $\kappa \in [-k_L, k_L]$ . To avoid representing the position operator  $\hat{x}$  in this basis, we work in the reduced lattice frame (cf. 1B) and rewrite the Floquet operator in the lattice frame as

$$U_{\text{lat}}(t_0 + T_F, t_0) = e^{-i2k_L \hat{x}} U_{\text{rlf}}(t_0 + T_F, t_0), \quad (\text{S27})$$

where

$$U_{\text{rlf}}(t_0 + T_F, t_0) = \mathcal{T} \exp\left(-\frac{i}{\hbar} \int_{t_0}^{t_0 + T_F} dt H_{\text{rlf}}(t)\right), \quad (\text{S28})$$

and  $\mathcal{T}$  denotes time-ordering. To compute  $U_{\text{rlf}}(t_0 + T_F, t_0)$ , we define a discrete time-grid with  $J$  equidistant grid points  $t_j = (j - 1/2) dt$  for  $j \in \{1, \dots, J\}$  and  $dt = T_F/J$ . For sufficiently small time-steps, we approximate

$$U_{\text{rlf}}(T) \simeq \prod_{j=1}^J \exp\left(-iH_{\text{rlf}}(t_j) dt / \hbar\right). \quad (\text{S29})$$

Next, we expand the Hamiltonian in the momentum basis  $|2n\hbar k_L + \hbar\kappa\rangle$

$$H_{\text{rlf}}(t_j) = \sum_{n \in \mathbb{Z}} \left( \left( \frac{(2n\hbar k_L + \hbar\kappa - p_L(t_j))^2}{2m} + \frac{V_0}{2} \right) |2n\hbar k_L + \hbar\kappa\rangle \langle 2n\hbar k_L + \hbar\kappa| + \frac{V_0}{4} (|2(n+1)\hbar k_L + \hbar\kappa\rangle \langle 2n\hbar k_L + \hbar\kappa| + \text{h.c.}) \right). \quad (\text{S30})$$

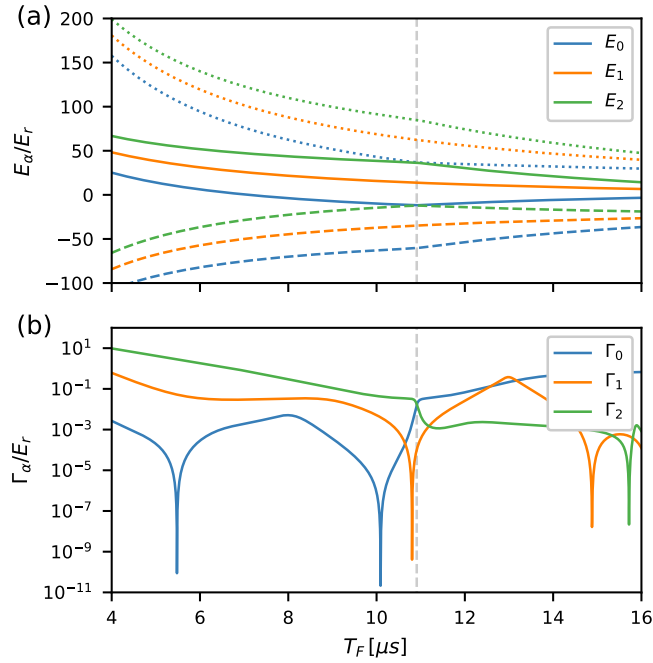


FIG. S3. (a) Quasienergies versus Floquet period at lattice depth  $V_0 = 50 E_r$ . The solid lines correspond to lattice site  $\ell = 0$ , the dashed lines to  $\ell = -1$  and the dotted lines to  $\ell = +1$ . The vertical dashed line marks the Floquet period where the energies of the lowest and the second excited Floquet bands show an avoided crossing. (b) First three Linewidths versus Floquet period at lattice depth  $V_0 = 50 E_r$ . Vertical dashed line marks the Floquet period where the linewidths of lowest and second excited Floquet bands show a real crossing, exactly where the real energies show an avoided crossing.

Note, that the average AC Stark shift  $V_0/2$  can be subtracted here for the computation of linewidths and states, or for the energies with AC stark shift suppression. To fully expand the Floquet operator (S27) in the momentum basis, we now consider the momentum shift operator  $e^{-i2k_L \hat{x}}$ , which takes the form

$$e^{-i2k_L \hat{x}} = \sum_{n \in \mathbb{Z}} |2(n-1)\hbar k_L + \hbar \kappa \rangle \langle 2n\hbar k_L + \hbar \kappa|. \quad (\text{S31})$$

The discretized Floquet operator can then be obtained by combining Eqs. (S27), (S30) and (S31). Note that we so far left the quasi-momentum undetermined, however the discretized Floquet operator belongs to the subspace of a specific quasi-momentum  $\kappa$ . The discretization is based on a time grid with  $J$  grid points and a momentum grid truncated at  $n \in [-N, N]$  with  $2N + 1$  grid points. This leads to a low-dimensional matrix, that can be efficiently constructed and diagonalized using standard libraries for scientific computing, however convergence in the discretization parameters  $J$  and  $N$  has to be ensured for accurate results. Truncating the momentum shift operator (S31) leads to a non-unitary matrix and subsequently to complex eigenvalues of the discretized Floquet operator  $U_{\text{lat}}(t_0 + T_F, t_0)$  of the form  $\lambda_n = \exp(-i\mathcal{E}_n T_F/\hbar) = \exp(-i(E_n - i\Gamma_n/2)T_F/\hbar)$ . From these eigenvalues we can determine the quasi-energies  $\mathcal{E}_n$  modulo  $2\pi\hbar/T_F$ . To compute the Floquet-Wannier-Stark energies  $\mathcal{E}_{\alpha,\ell}$ , the modulo operation needs to be reconstructed and furthermore the momentum state indices  $n$  need to be correctly mapped onto the band indices  $\alpha$ .

## B. Quasi-energy sorting

Finding the correct quasi-energyband sorting in Floquet systems is a common problem, since the band gaps are usually larger than the modulo operation, up to which one can obtain the quasi-energies. Hence sorting according to increasing energies  $E_n$  here will not result in the correct identification of  $n$  and  $\alpha$ . In the Wannier-Stark description of Bloch oscillation LMT pulses, it has been proven effective to sort according to increasing linewidths [5], which are usually much smaller than the remainder  $\text{Im}(\mathcal{E}_{\alpha,0}) = \Gamma_\alpha/2 \ll 2\pi\hbar/T_F$ . However this kind of sorting will fail real crossings of the linewidths of different Floquet bands and create artificial avoided crossings, which in the generalized case happens regularly. Nonetheless, in the limit of small Floquet periods  $T$ , sorting by increasing linewidths will give an unambiguous and correct mapping between the momentum state indices

$n$  and band indices  $\alpha$ . To resolve the issue of artificial avoided crossings we then impose an adiabaticity condition on the Floquet states of Systems with varied Floquet period  $T_F$  or lattice depth  $V_0$

$$\langle \phi_\alpha[\lambda] | \phi_\beta[\lambda + d\lambda] \rangle \simeq \delta_{\alpha\beta} \quad (\text{S32})$$

for  $d\lambda$  sufficiently small and  $\lambda = T_F$  or  $\lambda = V_0$ . Iteratively sorting by the condition (S32) on top of initially sorting by increasing linewidths results in the correct mapping between  $n$  and  $\alpha$  for all Floquet periods  $T_F$  and lattice depths  $V_0$ . It is important to note, that this sorting method can cause non-holonomic behavior [6]. Depending on which parameter is adiabatically varied and sorted by, the resulting state can be different. More precisely, the path taken in parameter space determines the resulting quantum state. Moreover, not only the eigenstate differs, as can for example be observed in the field of geometric phases, but also so does the eigenenergy. Therefore taking different paths in parameter space can result in occupying completely different eigenspaces, which is known as Cheon's anholonomies [6, 7]. This can be relevant for adiabatic preparation of the Floquet states, where multiple parameters are varied adiabatically in a specific order which corresponds to a specific path in parameter space.

---

[1] Note that, without loss of generality, we can set  $t_0 = 0$ . For the sake of consistency we keep track of  $t_0$  in the supplementary material, whereas in the main text we assume the initial time to be zero.

[2] M. Glück, F. Keck, A. R. Kolovsky, and H. J. Korsch, [Phys. Rev. Lett. \*\*86\*\*, 3116 \(2001\)](#).

[3] T. Rodzinka, E. Dionis, L. Calmels, S. Beldjoudi, A. Béguin, D. Guéry-Odelin, B. Allard, D. Sugny, and A. Gauguet, [Nature Communications \*\*15\*\*, 10281 \(2024\)](#).

[4] R. Grimm, M. Weidemüller, and Y. B. Ovchinnikov (Academic Press, 2000) pp. 95–170.

[5] F. Fitzek, J.-N. Kirsten-Siemß, E. M. Rasel, N. Gaaloul, and K. Hammerer, [Phys. Rev. Res. \*\*6\*\*, L032028 \(2024\)](#).

[6] M. Miyamoto and A. Tanaka, [Phys. Rev. A \*\*76\*\*, 042115 \(2007\)](#).

[7] T. Cheon, [Physics Letters A \*\*248\*\*, 285 \(1998\)](#).